Springer

KSME

Journal of Mechanical Science and Technology 26 (1) (2011) 1~7
www.springerlink.com/content/1738-494x
DOI 10.1007/s12206-011-0913-y

Multi-objective structural optimization of a hawt composite blade based on ultimate limit state analysis †

Weifei Hu[1], Insik Han[2], Sang-Chul Park[3] and Dong-Hoon Choi[4,*]

[1]*Graduate School of Mechanical Engineering, Hanyang University, Seoul, 133-791, Korea*
[2]*Engineer, Production Engineering Research Institute, LG Electronics Inc., Pyeongtaek-si, Gyeonggi-do, Korea*
[3]*Engineer, AbleMAX Inc., 2nd floor, JJ Building, 120-17, Samsung 2Dong, Kangnam Gu, Seoul, Korea*
[4]*Director, The Center of Innovative Design Optimization Technology (iDOT), Hanyang University, Seoul, 133-791, Korea*

(Manuscript Received January 11, 2011; Revised August 3, 2011; Accepted August 26, 2011)

Abstract

An extensively automated optimization procedure is presented for a horizontal axis wind turbine (HAWT) blade based on ultimate limit state analysis. Two composite materials named glass fiber reinforced plastic (GFRP) and carbon fiber reinforced plastic (CFRP) are applied with a multi-objective of blade cost and total mass. Laminate layer thickness, material type and orientation angle are tailored for the structural performance and subjected to three design constraints which are derived from analysis of ultimate strength, fatigue failure and critical deflection, respectively. Combining FEM analysis and an evolutionary algorithm, the proposed optimization process has dramatically reduced design cost and improved blade performance.

Keywords: Composite material; Multi-objective; Structural optimization; Ultimate limit state; Wind turbine blade

1. Introduction

With an ever-increasing demand for energy resources and concern over the global greenhouse effect, new energy-capture technologies with less carbon dioxide emissions have been in development and have advanced significantly in recent years. Wind turbine technology is one of such technology because it absorbs energy from the wind, which is a clean and renewable energy source. A modern horizontal axis wind turbine consists of a rotor, power train, nacelle, tower, foundation, and ground equipment station. The blade is one of the most important components in estimating the performance of a wind turbine. In this paper, the structural analysis and design optimization of a horizontal axis wind turbine (HAWT) blade is carried out based on ultimate limit state analysis.

For ultimate limit state analysis of the wind turbine, the following four types of analysis were performed where relevant [1]: analysis of ultimate strength, analysis of fatigue, stability analysis (buckling, etc.), and critical deflection analysis. M.M. Shokrieh et al. [2, 3] simulated the fatigue failure with the generalized material property degradation technique. Erik Lund et al. [4] studied the buckling analysis on only a wind turbine blade section, but not the whole blade. Many previous works concentrated mainly on certain aspects of ultimate limit state analysis and did not consider the cost or mass of the blade simultaneously. In this paper, three aspects of ultimate limit state analysis are investigated while three critical characteristics—laminate layer thickness, material type and orientation angle—are controlled to optimize the structural performance.

In general, the turbine blade is made of glass fiber reinforced plastic (GFRP) due to its low weight, high strength and stiffness, superior fatigue and corrosion properties. As blade dimension becomes larger, even GFRP cannot satisfy strength requirements, which leads to employment of lighter and stronger materials such as carbon fiber reinforced plastic (CFRP). Since the material cost of CFRP is much more than that of GFRP, the arrangement of GFRP and CFRP in composite layers has a significant effect on manufacturing cost. Thus both cost and mass are set to be a multi-objective function in this study.

To determine the optimal arrangement including material type (GFRP or CFRP), layer thickness and orientation angle of reinforcement in composite laminate, an advanced automatic optimization method is employed. The optimization routines and controls are held in a process integration and design optimization (PIDO) tool named PIAnO [5], which interfaces directly with a commercial finite element code

† This paper was recommended for publication in revised form by Associate Editor Jeonghoon Yoo
* Corresponding author. Tel.: +82 2 2220 0478, Fax.: +82 2 2291 4070
E-mail address: dhchoi@hanyang.ac.kr

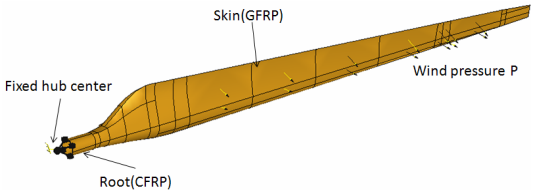

Fig. 1. Structural construction and state of load on the blade.

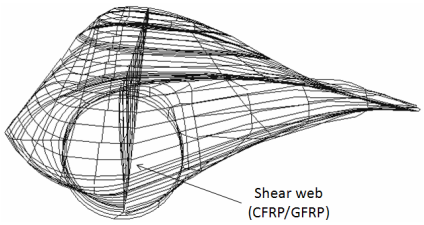

Fig. 2. Outer framework and shear web of the blade.

called SAMCEF [6]. When design variables, multi-objective function and constraints are set in PIAnO, the successive finite element solutions are automatically iterated upon until the optimum solution is achieved. According to manufacturing requirements, the layer thickness and orientation are usually discrete. To handle the discrete design problem, the evolutionary algorithm (EA) is used as an optimizer, which is a robust stochastic global optimization method.

2. FEM structural modeling

The configuration of an FEM model of CFRP/GFRP hybrid blade structure is shown in Figs. 1 and 2. The blade is composed of three parts: root, skin and shear web with the materials of CFRP, GFRP and a mixture of the two, respectively. Geometrical modeling is created in SAMCEF finite element software.

The blade is a 40 m long and has a 2 MW rated power. Airfoils for the root and the rear part of the blade are circle and NREL S-809, respectively. Twist distribution of airfoils along the blade is ignored for simplicity.

CFRP has lighter and stronger material performance than that of GFRP, but the unit volume cost of CFRP is ten times more expensive than that of GFRP, as suggested by A. Todoroki and Y. Kawakami [7]. According to the article [8], the shear webs prevent shear deformation and have the biggest influences on the bending modes of the blade. To compromise, the material distribution is shown in figures and shear web is made up of CFRP and GFRP layers, especially. Material properties of GFRP and CFRP are shown in Table 1.

The number of layers in root, skin and shear web are 20, 20 and 10, respectively. The design variables of the blade are layer thickness and reinforcement orientation angle of each layer as well as the material type, GFRP or CFRP, in shear web. For simplicity, all layer thicknesses in root are identical and all layer thicknesses in skin are the same too. The orientation angles are limited to 0°, ±45° and 90°. Considering the symmetric characteristics of composite laminate, the total design variables reduce from 150 to 27.

Table 1. Material properties of GFRP and CFRP.

Properties	GFRP	CFRP
E/GPa	56	90
υ	0.17	0.042
σ_{xt} /MPa	1447	1500
σ_{xc} /MPa	1447	1500
σ_{yt} /MPa	51	40
σ_{yc} /MPa	206	246
σ_{zt} /MPa	51	40
σ_{zc} /MPa	206	246
σ_{xy} /MPa	93	93
σ_{yz} /MPa	68	68
σ_{xz} /MPa	68	68
ρ /Kg/m^3	1500	1250
Cost/m^3	1	10

The analysis of the state of load on the wind turbine is intended to verify whether the turbine will withstand the action of load within an appropriate safety range. Jureczko et al. [9] investigated both aerodynamic loads and mass loads. Based on their paper [9] and the purpose of this research to simulate ultimate limit state, it is considered that the aerodynamic load can be simplified as wind pressure *P*, as shown in Fig. 1.

The mass, nodal displacement, stress, composite failure criterion (e.g. Tsai-Wu) ratio, etc. are provided by SAMCEF. All design variables are mapped by the mapping script function in PIAnO.

3. Ultimate limit state analysis

According to the IEC [1], four fields of analysis should be considered:

(1) Analysis of ultimate strength
(2) Analysis of fatigue failure
(3) Stability analysis (buckling, etc)
(4) Critical deflection analysis

The authors are currently investigating fields 1, 2 and 4, but this paper does not involve buckling analysis. Partial safety factors are used as factors to account for uncertainties of performance quantities.

3.1 Loading

The load used for analyzing ultimate limit state is a flapwise bending load derived from extreme wind speed of a recurrence period of 50 years. The turbine blade is categorized as class I [10] with the reference wind speed of 50 m/s. For simplicity, it is assumed that the aerodynamic load is imitated by the wind pressure *P* defined by Eq. (1).

$$P = \frac{1}{2}\rho V^2 C_p \tag{1}$$

where ρ, V and C_p represent air density, wind speed and pressure coefficient, respectively. The values ρ, V and C_p are 1.293 kg/m^3, 50 m/s and 2.0, respectively.

3.2 Partial safety factors

To assure safe design, the values for uncertainties and variability in loads and materials are taken into account by partial safety factors as defined in Eq. (2) and Eq. (3) [1] .

$$F_d = \gamma_f F_k \tag{2}$$

where F_d is the design value for the aggregated internal loads, γ_f is the partial safety factor for loads, and F_k is the characteristic value for the load.

$$f_d = \frac{1}{\gamma_m} f_k \tag{3}$$

where f_d are the design values for materials, f_k are the characteristic values of material properties, and γ_m are the partial safety factors for materials.

3.3 Analysis of ultimate strength

The ultimate strength of the blade is estimated by calculating maximum stress under the above load condition. The constraint about ultimate strength is represented by using the ratio of maximum stress σ_{max} to material strength σ_Y with partial safety factors as shown in Eq. (4).

$$\gamma_n \times \gamma_f \sigma_{\max} \le \frac{\sigma_Y}{\gamma_m} \tag{4}$$

where the value of γ_f for this load case is 1.35, that of γ_m for analysis of tensile or compression strength is 1.3, and that of γ_n for wind turbine class I is 0.9.

The strength ratio R that is used as a constraining function in the optimization process is the ratio between the applied stress and ultimate strength. It is based on the failure criterion of Tsai-Wu [11] and defined as the positive root of the following equation:

$$\left[F_{ij}\sigma_i\sigma_j\right]R^2 + \left[F_i\sigma_i\right]R - 1 = 0 \tag{5}$$

where F_i and F_{ij} are derived from the limit stresses listed in Table 1, σ_i, σ_j are the applied stress components, and all terms are cyclic in the i and j indices. Thus, the stress constraint is changed into the form in Eq. (6), where R could be obtained from SAMCEF directly, after combining the Tsai-Wu's failure criterion.

$$R = \frac{\sigma_{\max}}{\sigma_Y} \le \frac{1}{\gamma_m \gamma_n \gamma_f} \tag{6}$$

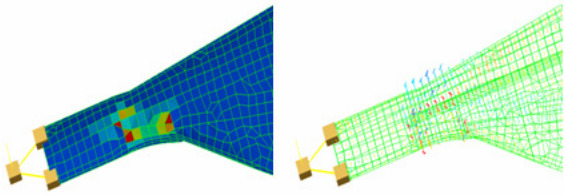

Fig. 3. Stress distribution: red elements (left) and red tensor arrows (right) indicate high stresses.

As the red spots show in Fig. 3, maximum stress occurs at the conjunction of the root and skin, indicating where the largest probability of failure is located.

3.4 Analysis of fatigue failure

Wind turbines are generally fatigue-critical machines, and the design of many of their components (especially blade) is dictated by fatigue considerations [12]. The fatigue behavior of the composite material in the blade structure can be defined by Eq. (7).

$$R = \frac{\sigma_{\max}}{\sigma_Y} = 1 - \beta \log_{10}(N) \tag{7}$$

where β is a parameter that varies for different materials. For the wind turbine composite blade materials, the value of β is 0.10632 [13]. N is the number of allowable cycles corresponding to peak working stress.

In order to increase the lifespan, the authors set the number of allowable cycles of the optimized blade to be larger than 10% of that of the initial one as shown in Eq. (8).

$$N = 10^{(1-R)/\beta} \ge 1.1 N_0 \tag{8}$$

where N_0 is the number of allowable cycles of initial blade.

3.5 Critical deflection analysis

The critical deflection is estimated by the tip deflection of the blade. As the load is applied onto the windward face of the blade, it deflects flapwise and the tip's deflection reaches its maximum. The constraint derived from critical deflection represents that the value of tip deflection w must be smaller than 5% of the blade length L [7] as shown in Eq. (9).

$$\gamma_n w\left(T_p, M_q, a_s\right) < 0.05L \tag{9}$$

where tip deflection w is a function of design variables for layer thickness T_p, material type M_q, and orientation angle a_s, p=1, 2, ..., 7; q=1, 2, ..., 5; s=1, 2, ..., 15. The value of γ_n for wind turbine class I is 0.9. The blade length L in this study is 40 m. Fig. 4 shows the meshed-blade deflection in the optimization process.

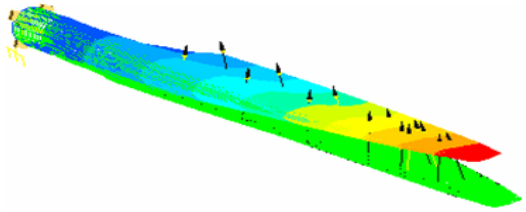

Fig. 4. A typical deflection of the finite element blade model.

4. Optimization problem

In this section, the authors describe how to use the design variable linking (DVL) technique to dramatically reduce the design variables. Then, the design objectives and constraints are formulated, and the final optimization model is given. The optimization iterative process and EA are also briefly introduced.

4.1 Design variable linking

Since there are 50 layers in this blade model and each layer has three design parameters (layer thickness, material type and orientation angle), the total number of design variables could reach 150. In order to reduce the number of design variables, real manufacturing conditions and symmetry of composite materials are considered and DVL is applied. The design variable linking technique can effectively reduce the number of design variables with which the optimizer must deal [14].

The numbers of layers in the root, shear web, and skin are represented by layers 1 to 20, layers 21 to 30 and layers 31 to 50, respectively. Because of laminate symmetry and simplicity considerations, design variable T_1 is linked to an identical layer thickness in the root; T_2 to T_6 are linked to layer thicknesses in the shear web; T_7 is linked to an identical layer thickness in the skin; a_1 to a_{15} are linked to orientation angles of layers in the root, shear web, and skin; and finally, M_1 to M_5 are linked to layer material types in the shear web. Thus there are only 27 design variables in total. The detail linking relationship between design variables and layer numbers is shown in Table 2.

Table 2. Design variables linking.

Design variables		Linking						
Thick-ness	DVs	T_1	T_2	T_3	T_4	T_5	T_6	T_7
	Layers (all)	1-20	21	22	23	24	25	31-50
			30	29	28	27	26	
Angle	DVs	a_1	a_2		a_3	a_4	a_5	
	Layers (root)	1	2		3	4	5	
		6	7		8	9	10	
		15	14		13	12	11	
		20	19		18	17	16	
	DVs	a_6	a_7		a_8	a_9	a_{10}	
	Layers (s.w.)	21	22		23	24	25	
		30	29		28	27	26	
	DVs	a_{11}	a_{12}		a_{13}	a_{14}	a_{15}	
	Layers (skin)	31	32		33	34	35	
		36	37		38	39	40	
		45	44		43	42	41	
		50	49		48	47	46	
Material	DVs	M_1	M_2		M_3	M_4	M_5	
	Layers (s.w.)	21	22		23	24	25	
		30	29		28	27	26	

4.2 Design objectives

The multi-objectives in this study are total mass and cost. The mass is obtained from the SAMCEF result batch file directly. The cost is a function of the layer thickness of all three parts of the blade and the arrangement of CFRP/GFRP in the shear web, given by Eq. (10).

$$Cost = 20w_1 f(2)T_1 + 2w_2 \sum_{q=1}^{5} f(M_q)T_{q+1} + 20w_3 f(1)T_7 \tag{10}$$

where T_1 is the CFRP layer thickness in the root, $T_{2\text{-}6}$ are the blended material layer thickness in the shear web, and T_7 is the GFRP layer thickness in the skin. M_q equals 1 or 2, which stands for the layer material being made up of GFRP or CFRP, correspondingly. w_1, w_2, and w_3 are volume-weighted coefficients for the root, shear web, and skin, respectively. $f(M_q)$ is the unit volume cost of GFRP and CFRP as follows.

$$f(M_q) = \begin{cases} 1 & \text{if } M_q = 1 \\ 10 & \text{if } M_q = 2 \end{cases}, \quad q = 1,2,...,5 \tag{11}$$

Due to varying costs of GFRT and CFRP in the market, the authors use rated cost to replace the true cost, which enlarges the usage range of this approach.

4.3 Design constraints and final optimization formulation

Three functional constraints are derived from the ultimate limit state analysis as shown by Eqs. (6), (8) and (9). Further side constraints are applied to the values of the design variables. The lower bound and upper bound of layer thickness T_p are $T_{p\text{-}low}$ and $T_{p\text{-}upp}$, respectively. In practice the fiber orientation angles of fiber-reinforced materials, e.g. GFRP and CFRP, are often limited to a discrete set such as 0°, ±45° and 90° in order to obtain a cost-effective design [15]. Thus, the final multi-objective optimization problem is formulated as follows:

Minimize $Cost + Mass$

Subject to

$$R = \frac{\sigma_{\max}}{\sigma_Y} \le \frac{1}{\gamma_m \gamma_n \gamma_f}$$

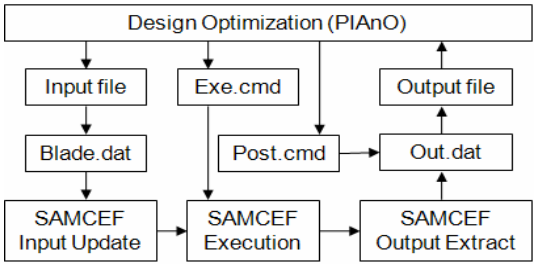

Fig. 5. Flow chart of the iterative optimization process.

$$
\begin{aligned}
&N = 10^{(1-R)/\beta} \geq 1.1N_0 \\
&\gamma_n w\left(T_p, M_q, a_s\right) < 0.05L \\
&T_{p\text{-}low} \leq T_p \leq T_{p\text{-}upp} \\
&M_q \in [1,2] \\
&a_s \in [-45,0,45,90]
\end{aligned} \tag{12}
$$

where p =1, 2, ..., 7; q =1, 2, ..., 5; s =1, 2, ..., 15.

4.4 Iterative process realization

Integration of SAMCEF to PIAnO tremendously reduces manual effort for iterative calculations required during design optimization because all data transfers are automated between SAMCEF and PIAnO as shown in Fig. 5. The design variables defined in the input file are mapped to Blade.dat. Then PIAnO controls the Exe.cmd to execute the SAMCEF. After execution, SAMCEF extracts the output to Out.dat. Finally, PIAnO controls the post-process command to read the necessary information, like maximal stress, mass, tip deflection, etc. to the output file. The iterative process repeats until the objective function is minimized while all the constraints are satisfied.

4.5 Optimization algorithm

As the design variables are all discrete and sensitivities of constraints are unavailable, the EA is selected as an optimizer, which is a class of direct, probabilistic search and optimization algorithm gleaned from the model of organic evolution. The main representatives of this computational paradigm are the genetic algorithm (GA), evolution strategy (ES) and evolutionary programming (EP) [16]. The EA parameters are shown in Table 3.

5. Results

Table 4 summarizes the simulated optimum values and initial values for design variables and objectives. From the table, the materials in shear web are all converged to GFRP which indicates that ten times higher cost of CFRP makes the optimizer choose GFRP satisfying the constraints, although CFRP is lighter and stronger than GFRP.

Table 3. EA parameter setting.

Population Size	20
Maximum Number of Generations	1000
Violated Constraint Limit	0.003
No. of Consecutive Generations without Improvement	20
Mutation probability	0.01
Selection Rate	0.15
Initial Seed Value	100

Table 4. Comparison of the initial and optimal results.

DVs	Initial	Optimum	DVs	Initial	Optimum
M_1	2	1	a_4	45	0
M_2	1	1	a_5	-45	90
M_3	2	1	a_6	0	90
M_4	1	1	a_7	45	45
M_5	2	1	a_8	-45	45
T_1	2.60	2.00	a_9	90	90
T_2	1.50	1.05	a_{10}	45	90
T_3	1.50	1.00	a_{11}	-45	0
T_4	0.80	0.70	a_{12}	90	45
T_5	0.80	0.75	a_{13}	45	0
T_6	1.30	1.10	a_{14}	90	90
T_7	2.60	2.05	a_{15}	0	90
a_1	-45	0	*cost*	384.5	292.8
a_2	45	-45	*mass*	6381.1	4925.3
a_3	90	0	Obj.	6765.6	5218.1

Table 4 also shows that all the layer thicknesses are reduced significantly. For example, the thickness of outer skin layers is reduced by 21.2%, which can dramatically decrease the total mass of the blade. Meanwhile, most of the fiber angle design variables, for instance a_1, a_3, a_4 in the root and a_{11}, a_{12}, a_{13} in the skin, are reduced from ±45° to 0°, and from 90° to 45° or 0°. This result is consistent with the reality that the root and skin are mainly subject to tensile/compressive stress during the ultimate limit state analysis and composite layer with a lower fiber angle can sustain larger tensile/compressive loads. The reduction ratios of cost and mass are 23.8% and 22.8%, respectively. The solutions steadily converge to optimum; Fig. 6 and Fig. 7 show the convergence history of cost and mass, respectively.

6. Conclusions and future work

In this study, a robust automated optimization process is presented to optimize the multi-objective structure of a HAWT blade based on ultimate limit state analysis. The same process could be applied in other industrial design and optimization problems combining the PIDO tools and the CAE tools. By performing ultimate strength analysis, the critical zone of the blade is obtained. Layer thickness, material type and orien-

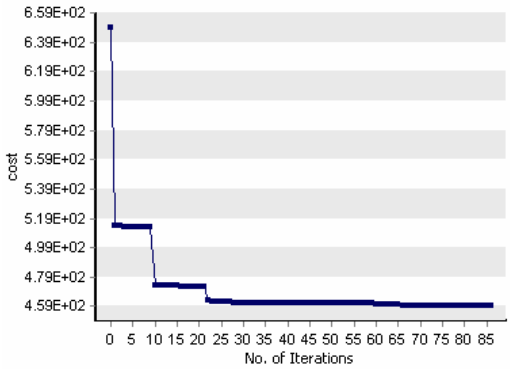

Fig. 6. Convergence history of the blade cost during the optimization process.

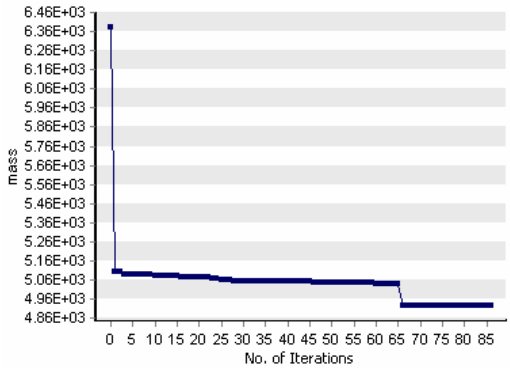

Fig. 7. Convergence history of the blade mass during the optimization process.

tation angle of GFRP/CFRP layers are optimized to reduce the total cost and mass. From the results, we can see that GFRP is chosen as the shear web material considering the large cost difference, which is reasonable in this design case. The optimal results show that the proposed optimization method improved the structural performance of the wind turbine blade, considering the conservative nature and uncertainties of performance quantities.

As a consequence of the minimum material design strategy, the structure of the modern HAWT blade is becoming thin-walled. Thus stability analysis, e.g., buckling problems, need to be studied and involved in the optimization process in the near future.

Acknowledgment

This work was supported by the NRF grant funded by the MEST (No. 2011-0016701). The authors also express gratitude to PIDOTECH Inc. that provides PIAnO software as a PIDO tool for this study.

Nomenclature

a_s : Fiber orientation angle
f_d : Design value for material strength
f_k : Characteristic value for material strength
w : Tip deflection
w_i : Volume-weighted coefficients, i =1, 2, 3
C_p : Pressure coefficient
F_d : Design value for loads
F_k : Characteristic value for loads
L : Blade length
M_q : Material type
N : Number of allowable cycles
N_0 : Number of allowable cycles of initial blade
P : Wind pressure
R : Strength ratio
T_p : Layer thickness
$T_{p\text{-}low}$: Lower bound of layer thickness
$T_{p\text{-}upp}$: Upper bound of layer thickness
V : Wind speed
β : Coefficient of fatigue property
γ_f : Partial safety factor for loads
γ_m : Partial safety factor for materials
γ_n : Partial safety factor for consequences of failure
ρ : Air density
σ_{max} : Maximum stress
σ_i, σ_j : Stress component
σ_Y : Material strength

References

[1] International Electrotechnical Commission, *IEC International Standard 61400-1 Part I: Design requirements*, Third Ed., Geneva, Switzerland (2005) 39-45.
[2] M. M. Shokrieh and R. Rafiee, Simulation of fatigue failure in a full composite wind turbine blade, *Composite Structure*, 74 (2006) 332-342.
[3] M. M. Shokrieh and L. B. Lessard, Progressive fatigue damage modeling of composite materials, Part I: Modeling, *Journal of Composite Materials*, 34 (13) (2000) 1056-80.
[4] E. Lund, L. Kuhlmeier and J. Stegmnn, Buckling optimization of laminated hybrid composite shell structures using discrete material optimization, *6th World Congress on Structural and Multidisciplinary Optimization*, Rio de Janeiro, Brazil (2005).
[5] PIDOTECH Inc., *PIAnO User's Manual*, Version 3.3, Seoul, Korea (2011).
[6] SAMTECH S. A., *SAMCEF User Manuals*, Version 11.0, Angleur-Liege, Belgium (2007).
[7] A. Todoroki and Y. Kawakami, Structural design for CF/GF hybrid wind turbine blade using multi-objective genetic algorithm and kriging model response surface method, *AIAA 2007 Conference and Exhibit*, California, USA (2007).
[8] C. Currin, T. Mitchell, M. D. Morris and D. Ylvi saker, Bayesian prediction of deterministic functions, with applications to the design and analysis of computer experiments, *Journal of the American Statistical Association*, 86 (416) (1991) 953-963.
[9] M. Jureczko, M. Pawlak and A. Meyk, Optimization of wind

turbine blade, *Journal of Materials Processing Technology*, 167 (2005) 463-471.
[10] International Electrotechnical Commission, *IEC International Standard 61400-1 Part I: Design requirements*, Third Ed., Geneva, Switzerland (2005) 21-22.
[11] J. R. Vinson and R. L. Sierakowski, *The behavior of structures composed of composite materials*, Second Ed., Kluwer Academic Publishers, Netherlands (2002).
[12] J. S. Rajadurai, T. Christopher, G. Thanigaiyarasu and B. N. Rao, Finite element analysis with an improved failure criterion for composite wind turbine blades, *Forsch Ingenieurwes*, 72 (2008) 193-207.
[13] J. F. Mandall, D. D. Samborsky and D. S. Cairns, *Fatigue of composite materials and substructures for wind turbine blades*, Sandia National Laboratories, Albuquerque, California, Sandia Report No. SAN2002-0771.
[14] G. N. Vanderplaats, *Numerical optimization techniques for engineering design*, Third Ed., Vanderplaats Research & Development, Inc., Colorado Spings (1999) 252-258.
[15] P. P. Camanho, C. G. Davila, S. T. Pinho and J. J. C. Remmers, *Mechanical response of composites*, Springer Press (2008) 244.
[16] B. Thomas, *Evolutionary algorithms in theory and practice,* Oxford University Press, Oxford (1996) 7.

Weifei Hu received his B.S. degree in Mechanical Engineering from Zhejiang University, China, in 2008. He then went on to receive his M.S. from Hanyang University, Korea, in 2010. He is currently a Ph.D candidate and research assistant at the University of Iowa. Mr. Hu's research interests are in the area of aerodynamic and structural optimization of wind turbine blade, and reliability-based design optimization.

Insik Han received a B.S. and M.S. degrees in Mechanical Engineering from Hanyang University, Korea, in 2006 and 2009, respectively. He is currently working for Production Engineering Research Institute at LG Electronics Inc., Korea. Mr. Han's research interests are in the area of product designs using practical optimization techniques such as DOE, Meta-Modeling, RA, RBDO, etc.

Sang-Chul Park received B.S degress in Mechanical Engineering from Suwon University, Korea, in 2008. He is currently working as technical enginner of ableMAX Inc., which is a CAE software distributor and CAE engineering company. He is charging with strucutural and dynamic analysis of wind turbine and automotive field.

Dong-Hoon Choi received a B.S. degree in Mechanical Engineering from Seoul National University in 1975. He then went on to receive his M.S. from KAIST, Korea, in 1977 and Ph.D degree from University of Wisconsin-Madison in 1986, respectively. Dr. Choi is currently a Professor at the School of Mechanical Engineering at Hanyang University in Seoul, Korea. He is currently the director of iDOT (the center of innovative design optimization technology). Prof. Choi's research interests are in the area of optimization techniques: developing MDO methodology, developing optimization techniques to ensure a reliability of optimum solution, and developing approximation optimization technique, etc.